

## Modification of Gastric Mucin Oligosaccharide Expression in Rhesus Macaques After Infection With *Helicobacter pylori*

CARA L. COOKE,<sup>\*,‡</sup> HYUN JOO AN,<sup>§</sup> JAEHAN KIM,<sup>||</sup> DON R. CANFIELD,<sup>¶</sup> JAVIER TORRES,<sup>#</sup> CARLITO B. LEBRILLA,<sup>§</sup> and JAY V. SOLNICK<sup>\*,‡,¶</sup>

<sup>\*</sup>Department of Internal Medicine and <sup>‡</sup>Department of Medical Microbiology & Immunology, Center for Comparative Medicine, and <sup>§</sup>Department of Chemistry, and <sup>||</sup>Department of Viticulture and Enology, University of California, Davis; <sup>¶</sup>California National Primate Research Center, Davis, California; and <sup>#</sup>Unidad de Investigación en Enfermedades Infecciosas, Hospital de Pediatría, IMSS, México City, Mexico

**BACKGROUND & AIMS:** *Helicobacter pylori* attaches to mucin oligosaccharides that are expressed on host gastric epithelium. We used the rhesus macaque model to characterize the effect of *H pylori* infection on gastric mucin oligosaccharides during acute and chronic infection. **METHODS:** Specific pathogen (*H pylori*)-free rhesus macaques were inoculated with *H pylori* J166. Biopsy specimens of the gastric antrum were obtained 2 and 4 weeks before and 2, 8, and 24 weeks after infection with *H pylori*. O-linked mucin oligosaccharides were released from gastric biopsy samples by  $\beta$ -elimination and profiled by matrix-assisted laser desorption/ionization mass spectrometry. Similar studies were performed on gastric biopsy samples from *H pylori*-infected and uninfected humans. Formalin-fixed, paraffin-embedded sections of rhesus antrum biopsy samples were stained with H&E, periodic acid-Schiff stain, and antibody to MUC5AC, the predominant mucin expressed in the stomach. **RESULTS:** *H pylori*-induced gastritis was accompanied by an acute and dramatic decrease in diversity and relative abundance of O-linked mucin oligosaccharides in the rhesus stomach, which largely recovered during the 24-week observation period. These variations in oligosaccharide abundance detected by mass spectrometry were reflected by changes in periodic acid-Schiff-positive material and expression of MUC5AC over time. Relatively few differences were seen in gastric mucin oligosaccharide composition between *H pylori*-infected and uninfected patients, which is consistent with the results in rhesus macaques because infection occurs in childhood. **CONCLUSIONS:** Acute *H pylori* infection is accompanied by a dramatic but transient loss in mucin oligosaccharides that may promote colonization and persistence.

Mucins are large glycoproteins that are the major structural component of the mucous gel layer that covers the epithelial surface and serves complex functions, which include not only cytoprotection<sup>1</sup> but also epithelial growth, development, and protection against microbial pathogens.<sup>2</sup> Mucins carry dense oligosaccharide side chains connected by O-glycosidic linkages at

serine or threonine residues. In the healthy human stomach, the major mucin proteins are secreted, including MUC5AC, which is localized to surface epithelial cells of the cardia, fundus, and antrum, and MUC6, which is expressed in the neck cells of the fundus and in antral glands. The membrane-associated mucins, MUC1 and MUC13, are also found in the stomach, although in lower abundance.

The gastric mucin population differs markedly in health and disease. In gastric precancerous lesions and in gastric cancer, there is altered expression of the usual gastric mucins, MUC5AC and MUC6, as well as metaplastic expression of the intestinal mucin, MUC2.<sup>3</sup> Altered expression of gastric mucins has also been found in response to infection with *Helicobacter pylori*, which is the major cause of peptic ulcer disease and an important factor in the development of gastric cancer.<sup>4</sup> Because the MUC5AC mucin displays Lewis b (Leb) and other fucosylated blood group antigens, which are thought to be the major receptors for *H pylori* in normal gastric tissue,<sup>5</sup> it is perhaps surprising that *H pylori* infection has sometimes been associated with reduced expression of MUC5AC.<sup>6-8</sup> However, contradictory findings have also been reported in different study populations.<sup>9,10</sup> These differences may result in part from the fact that analyses of gastric mucin are limited by *H pylori* strain diversity that exists in the human population and by the inability to study acute infection or even determine the duration of infection.

The nonhuman primate model offers the opportunity to study experimentally the effects of *H pylori* on expression of mucin oligosaccharides. Rhesus monkeys express mucins orthologous to human MUC5AC and MUC6 that share similar density, size, glycoforms, oligomeric structure, and tissue localization to those found in humans.<sup>11</sup> Rhesus macaques also express ABO and Le blood group antigens that serve as receptors for *H pylori*.<sup>11</sup> Socially

**Abbreviations used in this paper:** CFU, colony-forming units; Leb, Lewis b; MS, mass spectrometry; PAS, periodic acid-Schiff.

© 2009 by the AGA Institute

0016-5085/09/\$36.00

doi:10.1053/j.gastro.2009.04.014

housed rhesus monkeys are naturally infected with *H pylori*,<sup>12</sup> which supports the relevance of the model, but is an impediment to experimental infection. We therefore derived specific-pathogen (*H pylori*)-free macaques by isolating them at birth.<sup>12</sup> Experimental *H pylori* infection in macaques is characterized by a T helper cell 1-type inflammatory response, with infiltration of mononuclear and polymorphonuclear leukocytes that mimics the chronic active gastritis that is a hallmark of *H pylori* infection in humans.<sup>13</sup> Thus, the rhesus macaque can be used to study the role of gastric mucins in *H pylori* colonization and persistence in an ecologically relevant system.

We previously developed methods to analyze gastric mucin oligosaccharides from rhesus monkeys using matrix-assisted laser desorption/ionization (MALDI) mass spectrometry (MS).<sup>14</sup> Here we describe the use of MS and immunohistochemistry to determine the effect of experimental challenge with *H pylori* on rhesus monkey gastric mucins during acute and chronic infection. The results demonstrated a dramatic but transient decrease in mucin oligosaccharides in the rhesus monkey stomach after experimental challenge with *H pylori*, which was reflected in the amount of periodic acid-Schiff (PAS)-positive material and by changes in levels of the MUC5AC mucin. We speculate that *H pylori* modulates gastric mucin glycoproteins during acute infection to promote colonization and persistent infection.

## Materials and Methods

### Bacterial Strain and Culture

*H pylori* J166 preferentially colonizes rhesus monkeys and contains both a functional *cag* pathogenicity island and the s1m1 allele of the *vacA* cytotoxin.<sup>15</sup> Bacteria were cultivated on brucella agar or in brucella broth (Difco Laboratories, Detroit, MI) containing 5% bovine calf serum (GibcoBRL, Gaithersburg, MD) and antibiotics (trimethoprim, 5 mg/L; vancomycin, 10 mg/L; polymyxin B, 2.5 IU/L; amphotericin B, 4 mg/L; all from Sigma-Aldrich, St. Louis, MO), and incubated at 37°C with 5% CO<sub>2</sub>.

### Animals

Four male rhesus macaques 3 to 4 years of age were confirmed to be uninfected with *H pylori* using protocols described previously<sup>12</sup> and were housed at the California National Primate Research Center, which is accredited by the Association for the Assessment and Accreditation of Laboratory Animal Care. All procedures were approved by the primate center Research Advisory Committee and by the University of California, Davis, Chancellor's Animal Use and Care Administrative Advisory Committee.

### Animal Inoculations

A 50-mL liquid culture of *H pylori* J166 was cultivated overnight to an OD<sub>600</sub> of approximately 0.4, centrifuged, and resuspended in fresh brucella broth to an OD<sub>600</sub> of 1.0. Each monkey was inoculated orogastrically with 1 × 10<sup>9</sup> colony-forming units (CFU). The inoculum was examined by Gram's stain, urease, and oxidase tests to ensure a pure culture of *H pylori*.

### Biopsies and Quantitative Cultures

Each monkey underwent biopsy 2 and 4 weeks before *H pylori* inoculation and 2, 8, and 24 weeks postinoculation using a pediatric gastroscope (Pentax FG-16X, Montvale, NJ) with a 1.8-mm biopsy forceps. The procedure was performed under ketamine anesthesia (10 mg/kg of body weight intramuscularly) after an overnight fast. Seven antral biopsy specimens were collected from the stomach during each endoscopy. Two biopsy samples were placed in 250 μL brucella broth, homogenized with a sterile glass rod, and plated by serial dilution on brucella agar supplemented with 5% bovine calf serum and antibiotics. Plates were incubated at 37°C with 5% CO<sub>2</sub> for 5 to 6 days. *H pylori* colonies were identified in the conventional manner by colony morphology, microscopy, and biochemistry. CFU were counted, and CFU/g of tissue was determined for each monkey. The limit of detection was approximately 10<sup>2</sup> CFU/g.

### Histology and Immunohistochemistry

Two formalin fixed, paraffin-embedded biopsy samples from each monkey at each time point were sectioned (4 μm), deparaffinized, stained with H&E, and analyzed blindly for inflammation (mononuclear cells) and activity (polymorphonuclear leukocytes). Scores were generated as a composite of inflammation and activity according to the modified Sydney system.<sup>16</sup> For the PAS stain, sections were treated with the PAS Stain Kit (American Master Tech Scientific, Inc, Lodi, CA) according to the manufacturer's directions. For immunohistochemistry, sections were deparaffinized and treated with 3% hydrogen peroxide for 30 minutes. After rehydration, the slides were subjected to antigen retrieval in citrate buffer, pH 6.0, in a decloaker at 122°C. Slides were cooled to room temperature, washed in PBS, and blocked for 30 minutes. Slides were incubated overnight at room temperature with monoclonal anti-human gastric mucin antibody (1:2000 dilution of clone 45M1; Sigma-Aldrich), washed in PBS, and incubated for 1 hour at room temperature with biotinylated goat anti-mouse immunoglobulin G diluted 1:1000 in PBS + ova albumin. The Vectastain ABC Elite Kit (Vector Laboratories, Burlingame, CA) was used to detect all antibodies according to manufacturer's instructions. Slides were counterstained with hematoxylin before dehydration and mounting.

### Human Gastric Biopsy Samples

Gastric biopsy samples were obtained from the antrum of patients undergoing upper endoscopy at the General Hospital of the Instituto Mexicano del Seguro Social, México City, Mexico. Two biopsy samples were processed for *H pylori* culture as for macaques, and 2 biopsy samples were snap frozen in liquid nitrogen and stored at  $-80^{\circ}\text{C}$  until processed for MS. Samples were obtained from *H pylori* uninfected patients ( $n = 8$ ; mean age  $\pm$  SD,  $38.6 \pm 5.7$  years) and from patients infected with *H pylori* ( $n = 9$ ;  $37.9 \pm 5.4$  years), which was documented by culture, histology, and serology using methods previously described.<sup>17</sup> All *H pylori* strains were positive for the *cag* pathogenicity island, which was detected by polymerase chain reaction as previously described.<sup>18</sup> Informed consent was obtained from all participants in accordance with standard procedures approved by the local Institutional Review Board.

### Release of O-Linked Oligosaccharides From Gastric Biopsy Samples

Three biopsy samples were placed in 250  $\mu\text{L}$  of 70% ethanol, homogenized with a sterile glass rod, and dialyzed in Slide-A-Lyzer Mini Dialysis Units (10,000 MW cutoff; Pierce, Rockford, IL) against 2 L of nanopure  $\text{H}_2\text{O}$  at room temperature overnight. The material retained in the dialysis unit was lyophilized, and 1–3 mg was added to 500  $\mu\text{L}$  of alkaline borohydride solution (mixture of 1.0 mol/L sodium borohydride and 0.1 mol/L sodium hydroxide, Sigma-Aldrich). The mixture was incubated at  $42^{\circ}\text{C}$  for 12 hours in a water bath, and the reaction was neutralized by addition of 1.0 mol/L hydrochloric acid solution in an ice bath to destroy excess sodium borohydride.

### Oligosaccharide Purification by Porous Graphitized Carbon-Solid Phase Extraction

O-linked oligosaccharides released by reductive  $\beta$ -elimination were purified by solid phase extraction using a porous graphitized carbon cartridge (SPE-PGC; Alltech Associates, Deerfield, IL). The cartridge was washed with  $\text{H}_2\text{O}$  followed by 0.05% (vol/vol) trifluoroacetic acid in 80% acetonitrile (ACN)/ $\text{H}_2\text{O}$  (vol/vol). The solution of released oligosaccharide was loaded on the cartridge and washed with nanopure water at 1 mL/min to remove salts and buffer. O-linked glycans were eluted with ACN diluted in  $\text{H}_2\text{O}$  to 10%, 20%, or 40%, with 0.05% trifluoroacetic acid. Each fraction was collected and dried in a centrivap apparatus. Fractions were reconstituted in nanopure water prior to MS.

### Mass Spectrometric Analysis

Mass spectra were recorded on an external source HiResMALDI (IonSpec Corporation, Irvine, CA) equipped with a 7.0 Tesla magnet. The HiResMALDI was equipped with a pulsed Nd:YAG laser (355 nm). 2,5-Dihydroxy-

benzoic acid was used as a matrix (5 mg/100 mL in 50% ACN in  $\text{H}_2\text{O}$ ) for positive and negative mode, respectively. A saturated solution of NaCl in 50% ACN in  $\text{H}_2\text{O}$  was used as a cation dopant. The oligosaccharide solution (0.6  $\mu\text{L}$ ) was applied to the MALDI probe followed by matrix solution (0.6  $\mu\text{L}$ ). The sample was dried under a stream of air prior to MS.

A HiResESI (IonSpec Corporation, Irvine, CA) instrument equipped with a 9.4 Tesla magnet and Picoview nano-ESI source (New Objective, Woburn, MA) was used to obtain more sensitive detection of acidic oligosaccharides. Sample solutions for the nanoelectrospray source were delivered using a standard 6-port switching valve and an Eksigent 1D pump (Eksigent Technologies, Livermore, CA). Sample solutions were delivered with a flow rate of 250 nL/min composed of 0.1% formic acid in 50/50 water/ACN (vol/vol).

### Statistical Analysis

Bacterial density (CFU/g) was log transformed and analyzed by analysis of variance (ANOVA) with repeated measures. Pair-wise comparisons were performed using Student *t* test with the Bonferroni correction. Histologic analysis of inflammation, and of staining with PAS or antibody to MUC5AC, was analyzed using a mixed model analysis of variance (SAS proc. Mixed, version 9.2; SAS Inc, Cary, NC). Post hoc comparisons among time points were based on least squares means with the Bonferroni correction. The number of oligosaccharide compositions detected in rhesus monkey samples over time was analyzed by ANOVA with repeated measures. Post hoc comparisons among time points were based on Dunnett test, and pair-wise comparisons were performed using Student *t* test. Hierarchical cluster analysis was performed using HCE 3.5 software (<http://www.cs.umd.edu/hcil/hce>, University of Maryland, College Park, MD) for the systematic comparison of mass spectrometric data from *H pylori*-infected and uninfected samples. For the calculation, the absolute intensity of each peak was normalized by total ion intensity of spectra. Pearson correlation coefficient was used to calculate similarity, and each cluster was updated and drawn using the average group linkage method. The 2-tailed *P* value for statistical significance was .05.

## Results

### Quantitative *H pylori* Cultures

Two antral biopsy specimens were used to determine quantitative bacterial load from each monkey 2 and 4 weeks pre- and 2, 8, and 24 weeks postchallenge with *H pylori*. All monkeys were culture negative for *H pylori* before challenge and were stably infected with approximately  $10^6$  to  $10^7$  CFU/g of tissue throughout the observation period (Figure 1A). There were no statistically significant differences in *H pylori* bacterial load among the 3 postinfection time points.

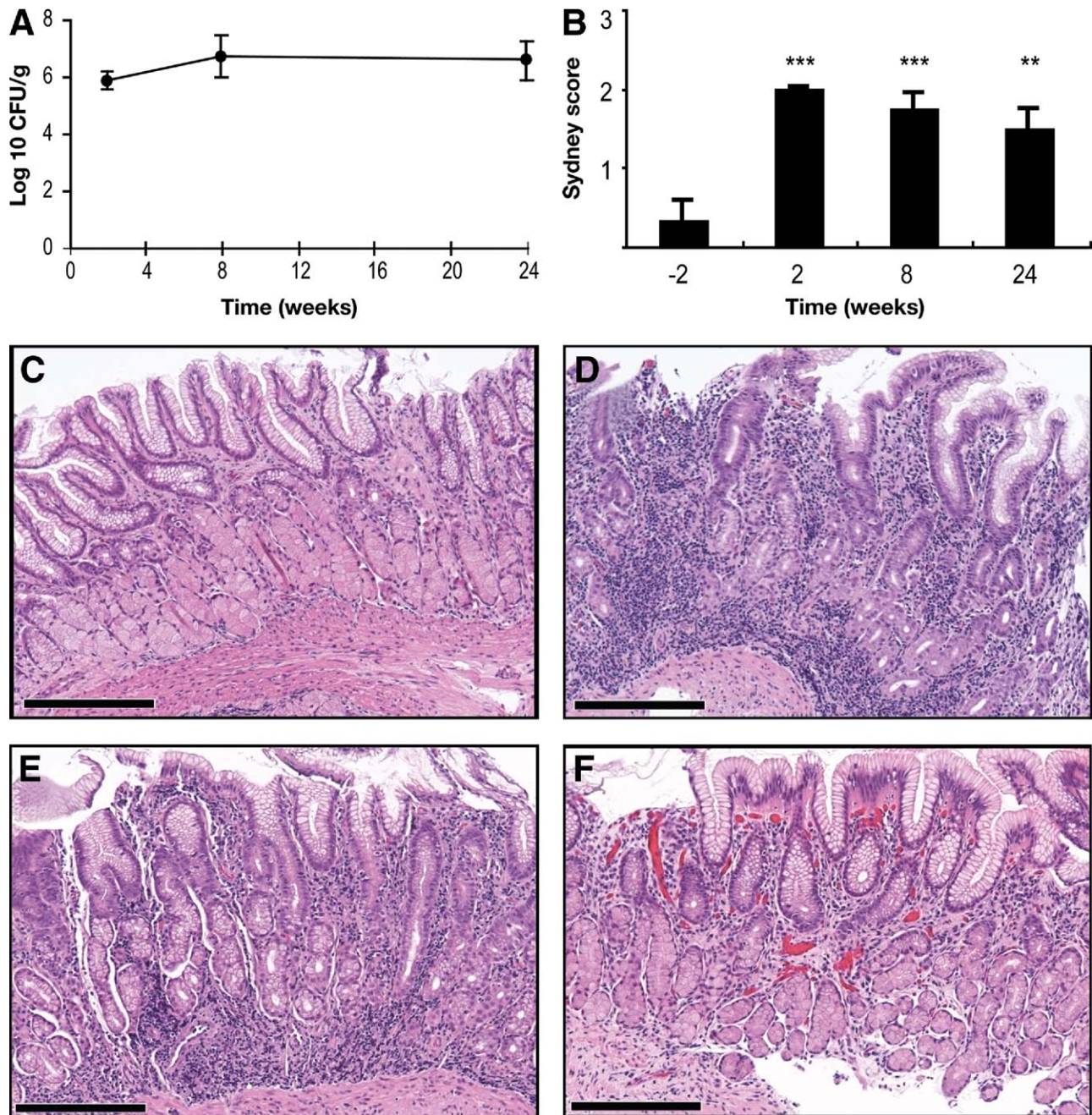


**Figure 1.** Quantitative *H pylori* culture and histopathology in antral gastric biopsy samples of rhesus macaques obtained 2, 8, and 24 weeks postinoculation. (A) *H pylori* bacterial load (mean  $\pm$  SE log<sub>10</sub> CFU/g) was stable among the 3 postinfection time points. (B) Mean ( $\pm$ SE) composite gastritis score (inflammation and activity) for all animals at 2 weeks preinoculation and 2, 8, and 24 weeks postinoculation was quantitated using the modified Sydney system. Gastritis was significantly increased after challenge as determined by a mixed model ANOVA. Pair-wise comparisons with prechallenge histopathology demonstrated a significant increase in gastritis at 2 ( $^{***}P < .001$ ), 8 ( $^{***}P < .001$ ), and 24 ( $^{***}P < .005$ ) weeks after challenge. (C–F) Representative photomicrographs of H&E-stained sections demonstrate that, compared with 2 weeks preinfection (C), there was a marked inflammatory response 2 (D), 8 (E), and 24 (F) weeks after *H pylori* challenge. At 2 weeks postinfection, the inflammation expanded the lamina propria, displacing both foveolar and glandular epithelial profiles. At 8- and particularly 24-weeks postinfection, although the inflammation persisted, its disruptive effect on gastric morphology was diminished. Scale bars, 200  $\mu$ mol/L.

### Histopathology

Biopsy sections from animals pre- and 2, 8, and 24 weeks postchallenge were stained with H&E and scored for inflammation (mononuclear cells) and activity (polymorphonuclear leukocytes) using the revised Sydney sys-

tem. Comparison of representative sections of gastric antrum before and after *H pylori* infection demonstrated a marked inflammatory response, consisting predominantly of plasma cells and lymphocytes, with some histiocytes and neutrophils superficially, and a more in-

tensely lymphocytic infiltration, sometimes follicular, in the deeper mucosa. Inflammation began as early as 2 weeks postinfection and persisted throughout the 24-week observation period, although it diminished over time (Figure 1C-F). At 2 weeks postinfection, the inflammatory infiltrate can be seen to expand the lamina propria, displacing or destroying both foveolar and glandular epithelial profiles. At 8 and particularly 24 weeks postinfection, although the inflammation persisted, its disruptive effect on gastric morphology was diminished. A composite Sydney score (Figure 1B) combining inflammation and activity was significantly increased after challenge ( $P < .0005$ ). Pair-wise comparisons with prechallenge histopathology demonstrated a significant increase in gastritis at 2 ( $P < .005$ ), 8 ( $P < .001$ ), and 24 ( $P < .005$ ) weeks after challenge. No evidence of gastric atrophy, intestinal metaplasia, or dysplasia was detected at any time point.

### MS Analysis of Mucin O-Linked Oligosaccharides

A mucin glycoprotein is composed of a peptide backbone that carries dense carbohydrate side chains connected by *O*-glycosidic linkages to serine or threonine residues. The *O*-glycosidic linkage is alkali labile, and thus the carbohydrate side chains can be released as oligosaccharide alditols by  $\beta$ -elimination with NaOH in the presence of NaBH<sub>4</sub>. These mucin *O*-linked oligosaccharides exhibit vast diversity because of the variety of monosaccharide compositions that make up the oligosaccharide, as well as to differences in length, branching, and linkages among the individual monosaccharides. However, all *O*-linked oligosaccharides are built on 1 of 8 core structures containing GalNAc in a nonreducing end. Because the instrument used in this study has high mass accuracy (<5 ppm with external calibration) and resolution (>100,000 full width at half height), the exact oligosaccharide composition with regard to hexose (Hex), *N*-acetylhexosamine (HexNAc), sialic acid, and fucose (Fuc) is readily determined solely based on mass. For example, an oligosaccharide with quasimolecular ion at  $m/z$  (mass/charge ratio) 1649.602 detected with a tolerance of 0.01 mass units must be 1 Fuc, 4 Hex, and 4 HexNAc. Accurate mass provides unambiguous assignment of glycan peaks, whereas the composition provides direct evidence for whether the oligosaccharide is *O*-linked (derived from mucins) or *N*-linked (nonmucinous glycoproteins). *O*-linked oligosaccharides were fractionated with solvents of varying polarity (10%, 20%, 40% ACN) to partition them into highly anionic and neutral components and then analyzed directly by MS in both the positive (cation) and negative (anion) modes. Because the 40% ACN fractions did not contain detectable glycans and the 10% and 20% fractions generated similar profiles of predominantly small, neutral oligosaccharides and some acidic structures, the 10% ACN fractions were used

for all analyses (Supplementary Figure 1). Assignments of selected oligosaccharide compositions were further confirmed by tandem MS using infrared multiphoton dissociation<sup>19</sup> as described in Supplementary Methods and Results and shown in Supplementary Figure 2.

### MS Profiles of O-Linked Mucin Oligosaccharides in Monkeys and Humans

We first examined oligosaccharide profiles in monkeys and humans that were uninfected with *H pylori*. Mucin core-type structures were identified that contained HexNAc and Hex residues, either with or without fucosylation (Supplementary Table 1), which were all consistent with *O*-linked, mucin-type oligosaccharides. Human samples yielded a greater number and more diversity of glycans than did samples from monkeys (Figure 2, Supplementary Table 1). Most of the 67 oligosaccharides detected in monkeys (86.6%) were found in at least 3 of 4 animals prior to infection (Figure 2A, Supplementary Table 1). Oligosaccharides detected in fewer than 3 animals typically had  $m/z$  greater than 2100, suggesting that the sensitivity for detection of larger mucin oligosaccharides may be reduced. In contrast to monkeys, human samples yielded a greater number of oligosaccharides (96 vs 67) and showed more biologic variability, with only 36.5% of the 96 oligosaccharides detected in all 8 human samples (Figure 2B, Supplementary Table 1). Humans and monkeys shared approximately 39% of oligosaccharide compositions (Figure 3, Supplementary Table 1).

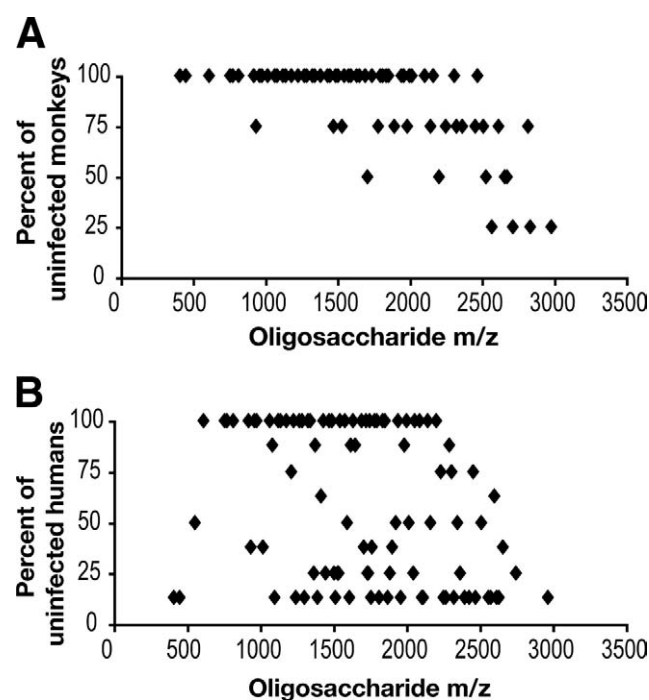


**Figure 2.** Oligosaccharide masses ( $m/z$ ) detected in 1 or more *H pylori*-uninfected monkeys (A) or humans (B). Oligosaccharide masses are plotted against the percentage of individuals in which they were detected.



BASIC-  
ALIMENTARY TRACT

Oligosaccharides were grouped according to whether they were common in humans and monkeys or unique to 1 species or another (Supplementary Table 1). Large highly fucosylated structures with mixtures of Lea and Leb epitopes were detected only in humans, although they expressed fewer anionic oligosaccharides. The sialic acid N-glycolylneuraminic acid (NeuGc) was detected only in monkeys (and NeuAc only in humans), which is consistent with inactivation of the gene encoding the enzyme CMP-N-acetylneuraminic acid (CMP-Neu5Ac) hydroxylase, thought to have occurred approximately 2.1 million years ago before the origin of present-day humans.<sup>20</sup>

**Effects of *H pylori* Infection on MS Profile of O-Linked Mucin Oligosaccharides**

To determine the effects of *H pylori* infection on mucin oligosaccharides, we first examined whether oligosaccharide profiles were stable over time in rhesus macaques before *H pylori* challenge. Spectra from each monkey 2 and 4 weeks prior to *H pylori* inoculation were compared for the presence or absence of oligosaccharide peaks and for the relative intensity of each peak normalized to the total ion intensity of the respective spectrum (Supplementary Figure 3). The glycan profiles were very similar for all animals between 2 and 4 weeks prior to inoculation, with correlation coefficients greater than 0.9. These data indicate that oligosaccharide profiles are both stable and reproducible over time.

We next compared the mean ( $\pm$ SD) number of oligosaccharides detected in the spectra of the 4 monkeys before challenge to that obtained 2, 8, and 24 weeks postchallenge with *H pylori* (Figure 4, Supplementary Tables 2 and 3). After 2 weeks of infection, there was a dramatic decline in mucin oligosaccharides, which could only be differentiated from background upon 5-fold concentration of the samples. Number of oligosaccharide compositions recovered partially 8 weeks after infection and returned to preinoculation levels by 24 weeks of infection.

Comparison of the normalized peak intensities for each animal at each time point using a heat map demonstrated that, although the number of peaks returned to preinoculation levels for all 4 monkeys, the peak intensities for 2 animals (animals C and D) differed from that detected prior to challenge (Figure 5). Thus, correlation coefficients of peak intensity between 4 weeks

←  
**Figure 3.** Hierarchical cluster analysis of oligosaccharide masses (*m/z*) detected in *H pylori* uninfected monkeys and humans was performed using HCE 3.5 software (<http://www.cs.umd.edu/hcil/hce>). Pearson correlation coefficient was used to calculate similarity, and each cluster was updated and drawn using the average group linkage method. The heat map displays the percentage of samples in which each oligosaccharide was detected as a gradient from 100% (red) to 50% (black) and to 0% (green).

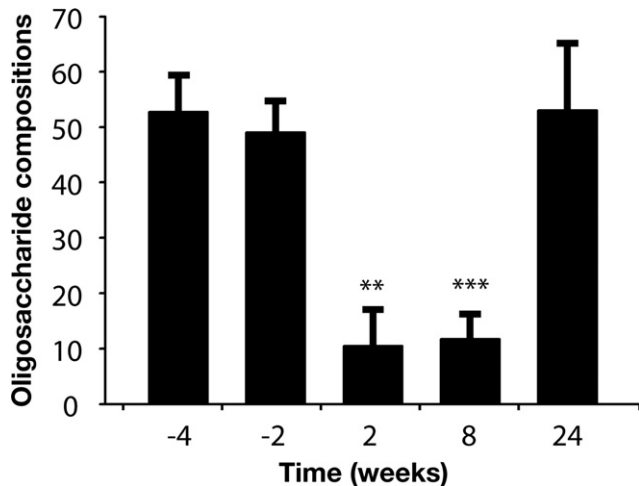


**Figure 4.** Mean ( $\pm$ SD) number of oligosaccharide compositions detected in mass spectra from 4 monkeys before (–4, –2 weeks) and after (2, 8, and 24 weeks) *H pylori* challenge. Mean number of peaks detected was significantly different among the 2-, 8-, and 24-week time points determined by ANOVA with repeated measures. Pair-wise comparisons with prechallenge profiles demonstrated a significant decrease in number of oligosaccharide compositions detected at 2 (\*\* $P < .005$ ) and 8 (\*\* $P < .001$ ) weeks after challenge.

before and 24 weeks after *H pylori* inoculation were high ( $R = 0.97$ ) for monkeys A and B but substantially lower for monkeys C ( $R = 0.61$ ) and D ( $R = 0.66$ ) (Figure 6), indicating that, although a similar number and type of oligosaccharides were detected 24 weeks after infection, in some cases the normalized absolute intensity differed from the preinoculation levels. Comparison of glycan profiles between patients infected or uninfected with *H pylori* showed relatively few differences (Supplementary Table 4), which is consistent with the monkey data because infection occurs in childhood and is chronic. Together, these results demonstrate that *H pylori* infection induces an acute and dramatic decrease in gastric mucin oligosaccharides, which largely recovers during chronic infection.

### PAS Stain

We next asked whether the changes in mucin-type oligosaccharides detected by MS were supported by loss of carbohydrate content in gastric tissue sections. PAS stains were performed on sections of gastric biopsy samples from monkeys before and after *H pylori* challenge. Sections from a representative monkey demonstrated a dramatic decrease in PAS staining 2 weeks after *H pylori* challenge that partially reversed over the subsequent 24-week observation period (Figure 7A–D). Quantitation of PAS-positive material was then performed on images of the stained sections using Image J software (<http://rsbweb.nih.gov/ij/>; National Institutes of Health, Bethesda, MD). Images were cropped to retain only gastric mucosa and split into red, green, and blue channels using the RGB split command. The green channel was used to calculate

the area of PAS-positive material because it provided maximal contrast between the PAS stain and the rest of the mucosa. The area of PAS-positive material was divided by total area of the mucosal epithelium for each image, and the results at each time point were averaged (Figure 7E). Percent PAS-positive material decreased markedly 2 weeks after *H pylori* challenge and subsequently increased, although the preinfection level was never recovered (Figure 7E). Statistical analysis by a mixed model ANOVA demonstrated a significant effect of time ( $P < .01$ ). Pair-wise comparisons with prechallenge biopsy samples showed that PAS-positive material was significantly decreased at 2 weeks ( $P < .05$ ) but not at 8 ( $P = .08$ ) or 24 ( $P = 0.16$ ) weeks after infection. These results support the MS data and suggest that mucin oligosaccharide expression at the gastric epithelial surface decreases during acute *H pylori* infection and partially recovers after 24 weeks.

### Immunohistochemistry

Immunohistochemical analysis of paraffin-embedded gastric biopsy samples was used to determine whether the decrease in mucin-type oligosaccharides correlated with changes in MUC5AC expression. Representative images prior to *H pylori* challenge showed marked MUC5AC-positive staining, predominantly in surface/foveolar cells (Figure 8A). MUC5AC expression decreased dramatically after 2 weeks of infection (Figure 8B) and then partially recovered over the 24-week observation period. Quantitation of MUC5AC staining using Image J

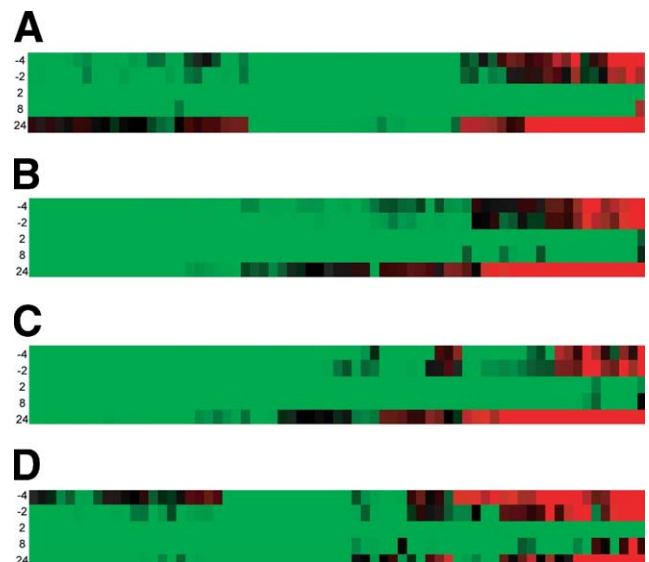


**Figure 5.** Hierarchical cluster analysis of absolute oligosaccharide peak intensities detected in each monkey (A–D) at each time point (–4 and –2, 2, 8, and 24 weeks) was performed using HCE 3.5 software (<http://www.cs.umd.edu/hcil/hce>). The heat map displays the absolute ion intensity of each oligosaccharide peak as a gradient from 100% (red) to 50% (black) and to 0% (green).

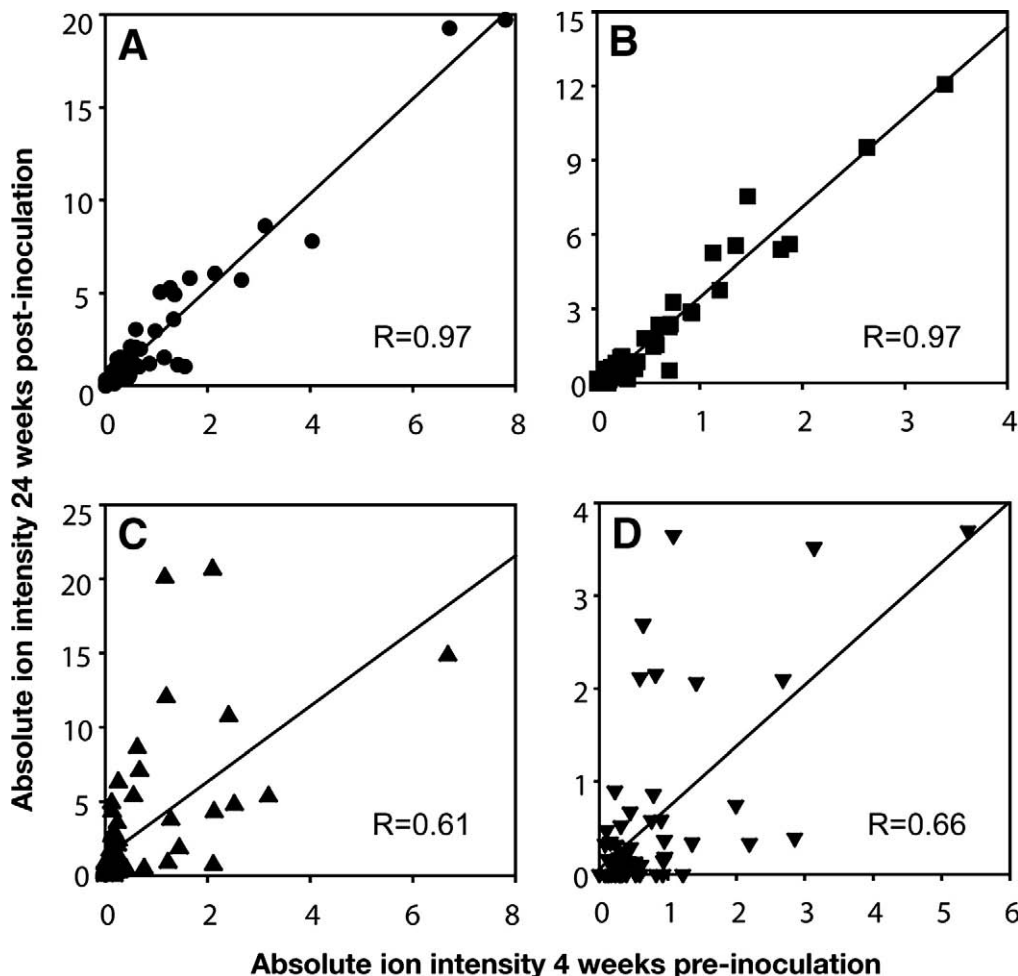


**Figure 6.** Correlation between mass spectra generated from each monkey (A–D) 4 weeks pre- and 24 weeks postinoculation with *H. pylori*. The absolute intensity of each oligosaccharide peak was first normalized by total ion intensity of the spectrum, and then Pearson *r* was used to calculate correlation between the profiles generated for each monkey.

software as for PAS (Figure 8E) showed that, although the overall trend was apparent, the time effect did not reach statistical significance ( $P = .18$ ).

## Discussion

Analysis of the effects of *H. pylori* on gastric mucins using human clinical samples has resulted in conflicting reports, probably because these studies are limited by *H. pylori* strain diversity that exists in the human population and by the inability to determine the duration of infection. For example, *H. pylori* has been associated with decreased MUC5AC and increased MUC6 expression in immunohistochemical analyses of gastric biopsy samples in some studies<sup>7</sup> but not others.<sup>9,10</sup> *H. pylori* also inhibits total mucin synthesis in gastric epithelial cell lines,<sup>8</sup> although mucin expression in transformed cells is not necessarily physiologic. Here, we demonstrate for the first time in vivo using the rhesus macaque model that gastric mucin oligosaccharide abundance and diversity dramatically decreases during the acute phase of infection and almost completely recovers to preinoculation levels during chronic infection, despite persistent inflammation

and constant bacterial levels. Marked changes at high resolution were seen by MS and confirmed by PAS staining and immunohistochemical analysis of MUC5AC. These findings emphasize that a major adaptation occurs between *H. pylori* and its mucosal niche during the first few weeks to months of infection, which later reaches a state of equilibrium. We have previously identified this to be a critical and dynamic period in studies of antigenic and phase variation in *H. pylori* outer membrane proteins<sup>21</sup> and host gene expression studies of antimicrobial innate immune effectors.<sup>22</sup> Mathematical models have also suggested that the first few months of *H. pylori* colonization are a dynamic period in relation to the host response.<sup>23</sup> Individual differences in bacterial or host adaptation, such as changes in expression of Lewis antigens,<sup>24,25</sup> may underlie the different glycan patterns among the monkeys (Figure 6). Because the human samples likely represent chronic colonization that has been present for decades, it is not surprising that few differences were found between *H. pylori*-infected and uninfected adults. The greater abundance and complexity of mucin oligosaccharides in humans compared with ma-

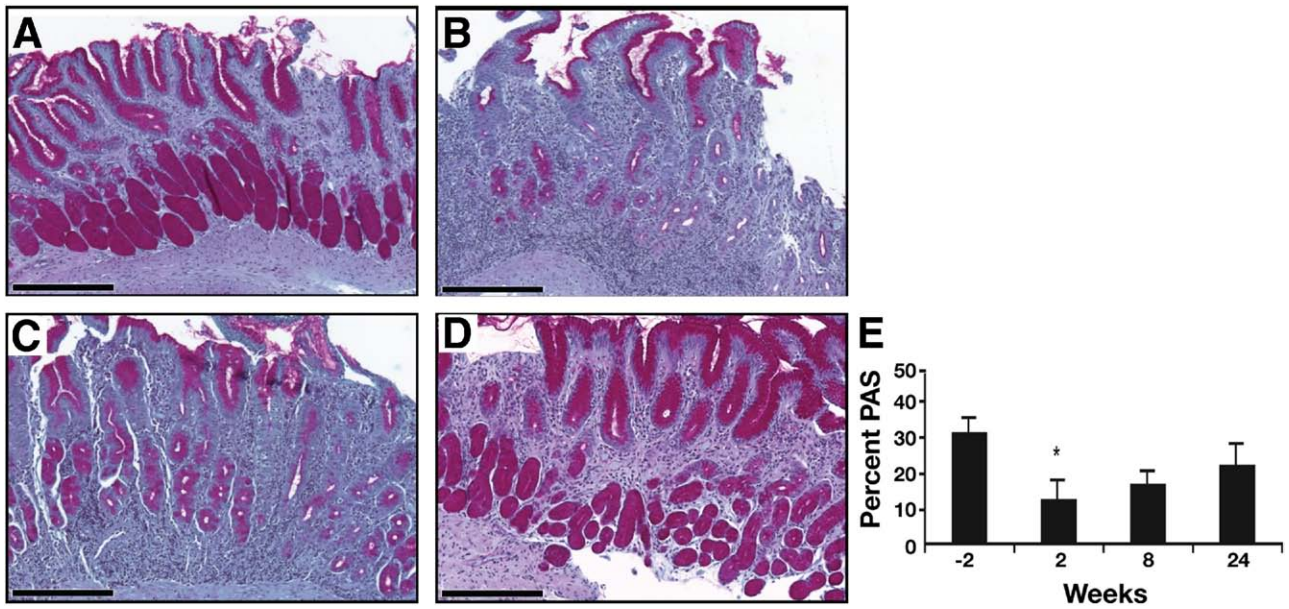


**Figure 7.** Representative photomicrographs of PAS-stained sections of gastric antrum from 2 weeks preinoculation (A) and 2 weeks (B), 8 weeks (C), and 24 weeks (D) postinoculation with *H pylori*. Percent of total area of gastric mucosa that stained PAS positive (bright magenta staining) was quantitated with Image J software (<http://rsbweb.nih.gov/ij/>) (E). Statistical analysis by a mixed model ANOVA demonstrated a significant effect of time ( $P < .01$ ). Pair-wise comparisons with prechallenge biopsy samples showed that PAS-positive material was significantly decreased at 2 weeks ( $P < .05$ ) but not at 8 ( $P = .08$ ) or 24 ( $P = .16$ ) weeks after infection. Scale bar, 200  $\mu\text{m}$ .

caques might be a species difference but may also result simply from the closed population of macaques from which the samples were drawn.

Previous work in the rhesus macaque demonstrated a transient decrease in mucosal Leb and increase in sialylation in rhesus macaques 1 to 4 weeks after *H*

*pylori* challenge.<sup>26</sup> Similarly, we found a transient loss of MUC5AC, which displays Leb and other fucosylated blood group antigens.<sup>5</sup> However, sialylated glycans were scarce in the pool of total mucin oligosaccharides, representing less than 3% of the total oligosaccharide abundance detected by MS, and no changes were found after

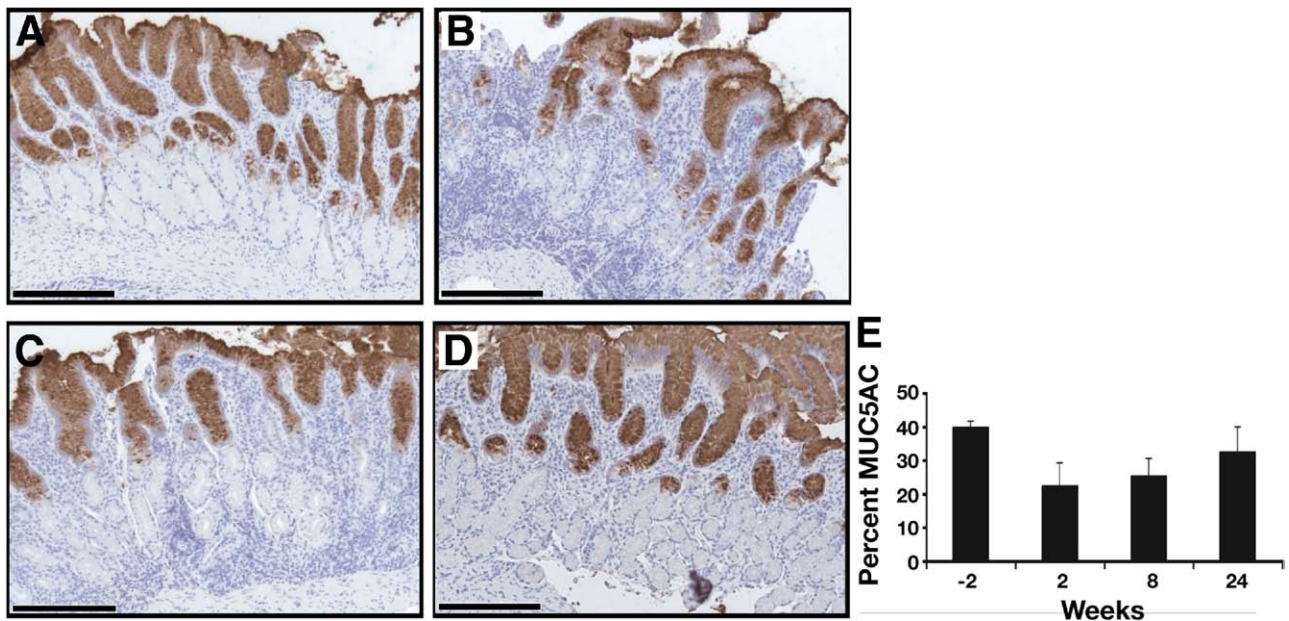


**Figure 8.** Representative photomicrographs of MUC5AC-stained sections of gastric antrum from 2 weeks preinoculation (A) and 2 weeks (B), 8 weeks (C), and 24 weeks (D) postinoculation with *H pylori*. Percent of total area of gastric mucosa that stained with anti-MUC5AC antibody (brown staining) was quantitated with Image J software (<http://rsbweb.nih.gov/ij/>) (E). Quantitation of MUC5AC staining using Image J software showed that, although the overall trend was apparent, the time effect did not reach statistical significance ( $P = .18$ ). Scale bars, 200  $\mu\text{m}$ .

infection. Thus, it appears that sialylated glycans are uncommon in the gastric mucosa, and changes in sialylation may be detectable only with immunohistochemistry or other highly sensitive methods.

The mechanisms by which *H pylori* might alter expression of mucin oligosaccharides are unknown. Cholera toxin and *Entamoeba histolytica* trophozoites enhance the secretion of preformed and newly synthesized mucin glycoproteins, which may deplete the protective mucus layer and facilitate pathogenesis.<sup>27,28</sup> On the other hand, the available evidence suggests that *H pylori* actually down-regulates mucin exocytosis.<sup>29</sup> Transcriptional changes in mucin expression occur commonly in response to bacterial products such as lipopolysaccharides, neutrophil elastase, interleukin-1 $\beta$ , and other inflammatory mediators, but, in contrast to our findings, the expression is typically induced.<sup>30</sup> Reports of *H pylori* protease, glycosulfatase, and neuraminidase activities that degrade gastric mucins<sup>31,32</sup> are controversial. Finally, *H pylori* may alter expression of genes involved in glycan synthesis, such as induction of a GlcNAc transferase essential for the biosynthesis of Lewis antigens.<sup>33</sup> Because the reduction in PAS was more striking than that for MUC5AC, which was detected with an antibody thought to recognize the peptide backbone,<sup>34</sup> we speculate that *H pylori* induces changes in mucin glycosylation during acute infection.

The dramatic changes in mucin oligosaccharides we observed during acute *H pylori* infection could represent a pathogenic mechanism for bacterial persistence, a host defense, or both. On the one hand, depletion of mucins bearing fucosylated blood group antigens and other glycan receptors might enhance bacterial access to the epithelial surface and promote chronic infection. Once the epithelial layer is colonized, there may no longer be any microbial benefit to mucin depletion, and, in fact, the mucin layer may then be protective. On the other hand, the decreased oligosaccharide content during acute infection could be a host defense, much like MUC1 that is thought to act as a "releasable decoy ligand" for *H pylori* that, upon bacterial adherence, is cleaved by host cell proteases and released from the host cell surface.<sup>35</sup> Because the mucin oligosaccharides recover almost to preinoculation levels, despite persistent inflammation and constant bacterial load, we speculate that the changes seen during acute infection are likely critical for bacterial colonization and persistence.

### Supplementary Data

Note: To access the supplementary material accompanying this article, visit the online version of *Gastroenterology* at [www.gastrojournal.org](http://www.gastrojournal.org), and at doi: 10.1053/j.gastro.2009.04.014.

### References

- Laine L, Takeuchi K, Tarnawski A. Gastric mucosal defense and cytoprotection: bench to bedside. *Gastroenterology* 2008;135:41–60.
- Lievín-Le Moal V, Servin AL. The front line of enteric host defense against unwelcome intrusion of harmful microorganisms: mucins, antimicrobial peptides, and microbiota. *Clin Microbiol Rev* 2006;19:315–337.
- Hollingsworth MA, Swanson BJ. Mucins in cancer: protection and control of the cell surface. *Nat Rev Cancer* 2004;4:45–60.
- Kusters JG, van Vliet AH, Kuipers EJ. Pathogenesis of *Helicobacter pylori* infection. *Clin Microbiol Rev* 2006;19:449–490.
- Van de Bovenkamp JH, Mahdavi J, Korteland-Van Male, et al. The MUC5AC glycoprotein is the primary receptor for *Helicobacter pylori* in the human stomach. *Helicobacter* 2003;8:521–532.
- Beil W, Enss ML, Muller S, et al. Role of *vacA* and *cagA* in *Helicobacter pylori* inhibition of mucin synthesis in gastric mucous cells. *J Clin Microbiol* 2000;38:2215–2218.
- Byrd JC, Yan P, Sternberg L, et al. Aberrant expression of gland-type gastric mucin in the surface epithelium of *Helicobacter pylori*-infected patients. *Gastroenterology* 1997;113:455–464.
- Byrd JC, Yunker CK, Xu QS, et al. Inhibition of gastric mucin synthesis by *Helicobacter pylori*. *Gastroenterology* 2000;118:1072–1079.
- Kang HM, Kim N, Park YS, et al. Effects of *Helicobacter pylori* infection on gastric mucin expression. *J Clin Gastroenterol* 2008;42:29–35.
- Marques T, David L, Reis C, et al. Topographic expression of MUC5AC and MUC6 in the gastric mucosa infected by *Helicobacter pylori* and in associated diseases. *Pathol Res Pract* 2005;201:665–672.
- Linden S, Boren T, Dubois A, et al. Rhesus monkey gastric mucins: oligomeric structure, glycoforms and *Helicobacter pylori* binding. *Biochem J* 2004;379:765–775.
- Solnick JV, Canfield DR, Yang S, et al. Rhesus monkey (*Macaca mulatta*) model of *Helicobacter pylori*: noninvasive detection and derivation of specific-pathogen-free monkeys. *Lab Anim Sci* 1999;49:197–201.
- Mattapallil JJ, Dandekar S, Canfield DR, et al. A predominant Th1 type of immune response is induced early during acute *Helicobacter pylori* infection in rhesus macaques. *Gastroenterology* 2000;118:307–315.
- Cooke CL, An HJ, Kim J, et al. Method for profiling mucin oligosaccharides from gastric biopsy of rhesus monkeys with and without *Helicobacter pylori* infection. *Anal Chem* 2007;79:8090–8097.
- Solnick JV, Hansen LM, Canfield DR, et al. Determination of the infectious dose of *Helicobacter pylori* during primary and secondary infection in rhesus monkeys (*Macaca mulatta*). *Infect Immun* 2001;69:6887–6892.
- Dixon MF, Genta RM, Yardley JH, et al. Classification and grading of gastritis. The updated Sydney System. International Workshop on the Histopathology of Gastritis, Houston 1994. *Am J Surg Pathol* 1996;20:1161–1181.
- Camorlinga-Ponce M, Flores-Luna L, Lazcano-Ponce E, et al. Age and severity of mucosal lesions influence the performance of serologic markers in *Helicobacter pylori*-associated gastroduodenal pathologies. *Cancer Epidemiol Biomarkers Prev* 2008;17:2498–2504.
- Tummuru MK, Cover TL, Blaser MJ. Cloning and expression of a high-molecular-mass major antigen of *Helicobacter pylori*: evidence of linkage to cytotoxin production. *Infect Immun* 1993;61:1799–1809.
- Lancaster KS, An HJ, Li B, et al. Interrogation of N-linked oligosaccharides using infrared multiphoton dissociation in FT-ICR mass spectrometry. *Anal Chem* 2006;78:4990–4997.

20. Chou HH, Hayakawa T, Diaz S, et al. Inactivation of CMP-N-acetylneuraminic acid hydroxylase occurred prior to brain expansion during human evolution. *Proc Natl Acad Sci U S A* 2002;99:11736–11741.
21. Solnick JV, Hansen LM, Salama NR, et al. Modification of *Helicobacter pylori* outer membrane protein expression during experimental infection of rhesus macaques. *Proc Natl Acad Sci U S A* 2004;101:2106–2111.
22. Hornsby MJ, Huff JL, Kays RJ, et al. *Helicobacter pylori* induces an antimicrobial response in rhesus macaques in a cag pathogenicity island-dependent manner. *Gastroenterology* 2008;134:1049–1057.
23. Blaser MJ, Kirschner D. Dynamics of *Helicobacter pylori* colonization in relation to the host response. *Proc Natl Acad Sci U S A* 1999;96:8359–8364.
24. Wirth HP, Yang M, Sanabria-Valentin E, et al. Host Lewis phenotype-dependent *Helicobacter pylori* Lewis antigen expression in rhesus monkeys. *FASEB J* 2006;20:1534–1536.
25. Nilsson C, Skoglund A, Moran AP, et al. Lipopolysaccharide diversity evolving in *Helicobacter pylori* communities through genetic modifications in fucosyltransferases. *PLoS ONE* 2008;3:e3811.
26. Linden S, Mahdavi J, Semino-Mora C, et al. Role of ABO secretor status in mucosal innate immunity and *H pylori* infection. *PLoS Pathog* 2008;4:e2.
27. Chadee K, Keller K, Forstner J, et al. Mucin and nonmucin secretagogue activity of *Entamoeba histolytica* and cholera toxin in rat colon. *Gastroenterology* 1991;100:986–997.
28. Leitch GJ. Cholera enterotoxin-induced mucus secretion and increase in the mucus blanket of the rabbit ileum in vivo. *Infect Immun* 1988;56:2871–2875.
29. Micots I, Augeron C, Laboisie CL, et al. Mucin exocytosis: a major target for *Helicobacter pylori*. *J Clin Pathol* 1993;46:241–245.
30. Li JD, Dohrman AF, Gallup M, et al. Transcriptional activation of mucin by *Pseudomonas aeruginosa* lipopolysaccharide in the pathogenesis of cystic fibrosis lung disease. *Proc Natl Acad Sci U S A* 1997;94:967–972.
31. Sidebotham RL, Batten JJ, Karim QN, et al. Breakdown of gastric mucus in presence of *Helicobacter pylori*. *J Clin Pathol* 1991;44:52–57.
32. Suerbaum S, Friedrich S. *Helicobacter pylori* does not have a hap mucinase gene that is quasi-identical to the *Vibrio cholerae* hap gene. *Mol Microbiol* 1996;20:1113–1114.
33. Marcos NT, Magalhaes A, Ferreira B, et al. *Helicobacter pylori* induces  $\beta$ 3GnT5 in human gastric cell lines, modulating expression of the SabA ligand sialyl-Lewis x. *J Clin Invest* 2008;118:2325–2336.
34. Lidell ME, Bara J, Hansson GC. Mapping of the 45M1 epitope to the C-terminal cysteine-rich part of the human MUC5AC mucin. *FEBS J* 2008;275:481–489.
35. McGuckin MA, Every AL, Skene CD, et al. Muc1 mucin limits both *Helicobacter pylori* colonization of the murine gastric mucosa and associated gastritis. *Gastroenterology* 2007;133:1210–1218.

---

Received January 13, 2009. Accepted April 9, 2009.

#### Reprint requests

Address requests for reprints to: Jay V. Solnick, MD, PhD, Center for Comparative Medicine, University of California-Davis, Davis, California 95616. e-mail: [jvsolnick@ucdavis.edu](mailto:jvsolnick@ucdavis.edu); fax: (530) 752-7914.

#### Conflicts of interest

The authors disclose no conflicts.

#### Funding

Supported by Public Health Service Grants AI42081, GM490077, and NRSA AI60555.

## Supplementary Methods

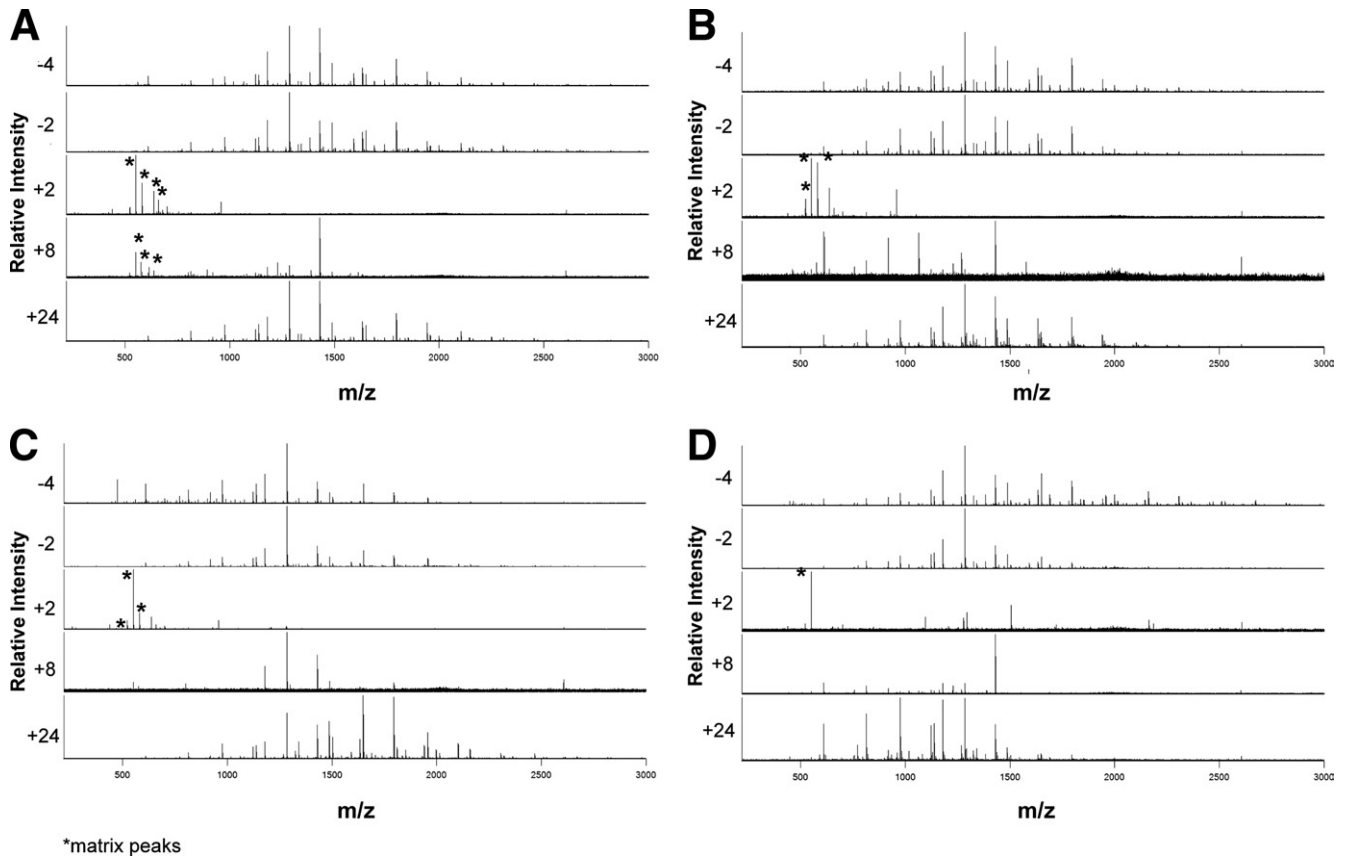
### *Structural Elucidation of Oligosaccharides Using Infrared Multiphoton Dissociation*

Tandem mass spectrometry was performed using structural elucidation of oligosaccharides using infrared multiphoton dissociation (IRMPD) to determine the general structures of selected oligosaccharides, which allowed for complete fragmentation of the ion of interest. The ion of interest was readily selected in the analyzer with the use of an arbitrary-wave form generator and a frequency synthesizer. A continuous wave Parallax CO<sub>2</sub> laser (Waltham, MA) with 20-W maximum power and 10.6- $\mu$ m wavelength was installed at the rear of the magnet and was used to provide the photons for IRMPD. The laser beam diameter was 6 mm as specified by the manufacturer. The laser beam was expanded to  $\sim$ 12 mm by means of a 2 $\times$  beam expander (Synrad, Mukilteo, WA) to ensure complete irradiation of the ion cloud through the course of the experiment. The laser was aligned and directed to the center of the ICR cell through a BaF<sub>2</sub> window (Bicron Corporation, Newbury, OH). Photon irradiation time was optimized to produce the greatest number and abundance of fragment ions. The laser was operated at an output of approximately 13 W.

## Supplementary Results

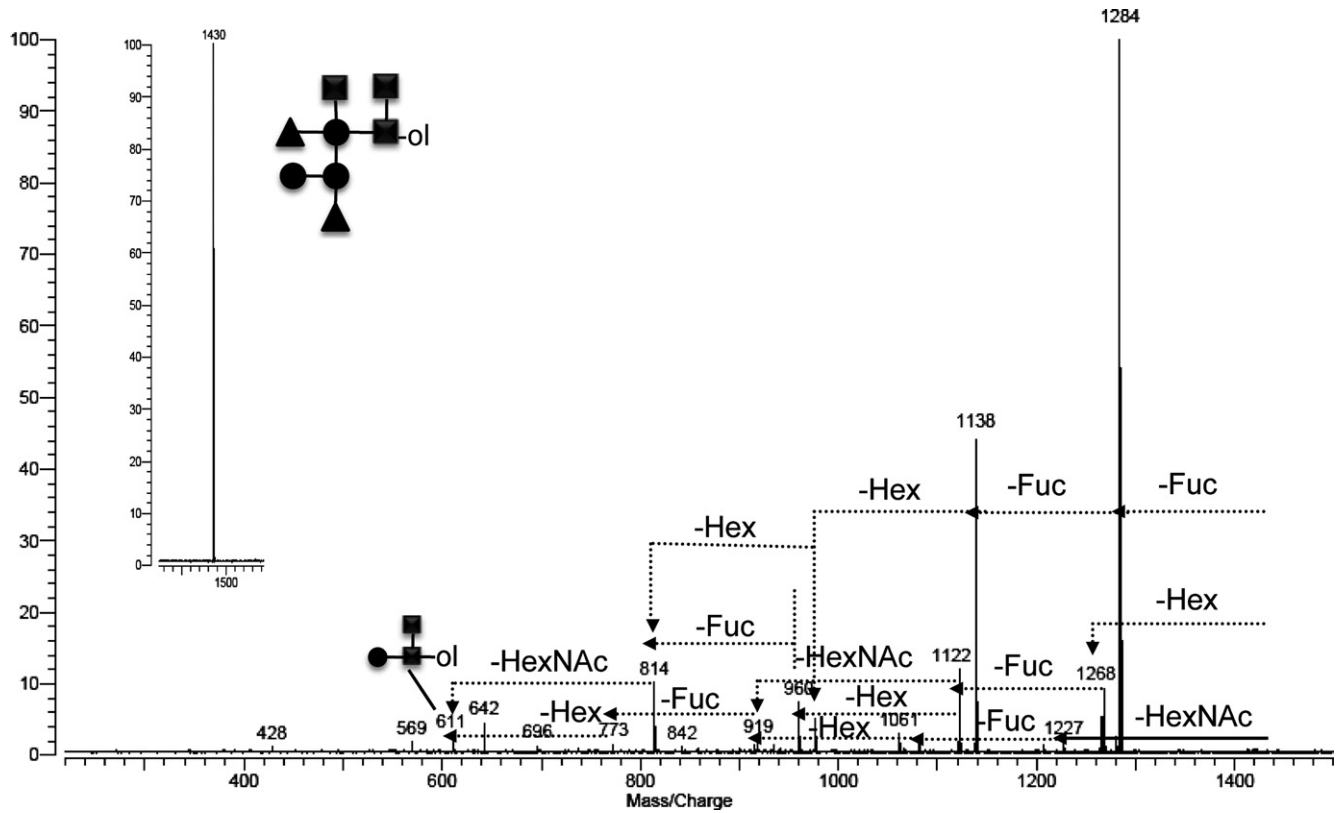
### *Structural Elucidation of Oligosaccharides Using Infrared Multiphoton Dissociation*

To confirm glycan composition and to obtain structural information, selected ions were subjected to tandem mass spectrometry (MS) using infrared multiphoton dissociation (IRMPD) structural elucidation of oligosaccharides. For example, IRMPD analysis of the ion at  $m/z$  1430.528 ( $[M+Na]^+$ ), corresponding to 3 hexose (Hex), 3 N-acetylhexosamine (HexNAc), and 2 fucose (Fuc), yielded loss of 2 consecutive Fuc from the quasi-molecular ion ( $m/z$  1430 $\rightarrow$ 1284 $\rightarrow$ 1138), indicating the presence of 2 Fuc residues with nonreducing terminal positions and at least 1 branched point (Supplementary Figure 2). Similarly, the loss of Hex ( $m/z$  1268) and HexNAc ( $m/z$  1227) indicated that these residues were also present as nonreducing termini. There was no further Hex loss from  $m/z$  1268, suggesting that the 2 Hex residues were internal. The ion at  $m/z$  611 corresponded to 1 Hex, 1 HexNAc, and HexNAc-ol, which identified the known trisaccharide core structure for mucin-type oligosaccharides. Thus, the primary sequence of the ion  $m/z$  1430 based on the tandem MS was determined (Supplementary Figure 2, *inset*).



\*matrix peaks

Supplementary Figure 1. Mass spectra generated from each animal at each time point.



**Supplementary Figure 2.** Structural elucidation of oligosaccharides using infrared multiphoton dissociation (IRMPD) analysis of the ion at  $m/z$  1430.528 ( $[M+Na]^+$ ). The primary sequence of the ion  $m/z$  1430 based on the tandem MS is displayed in the *inset*.

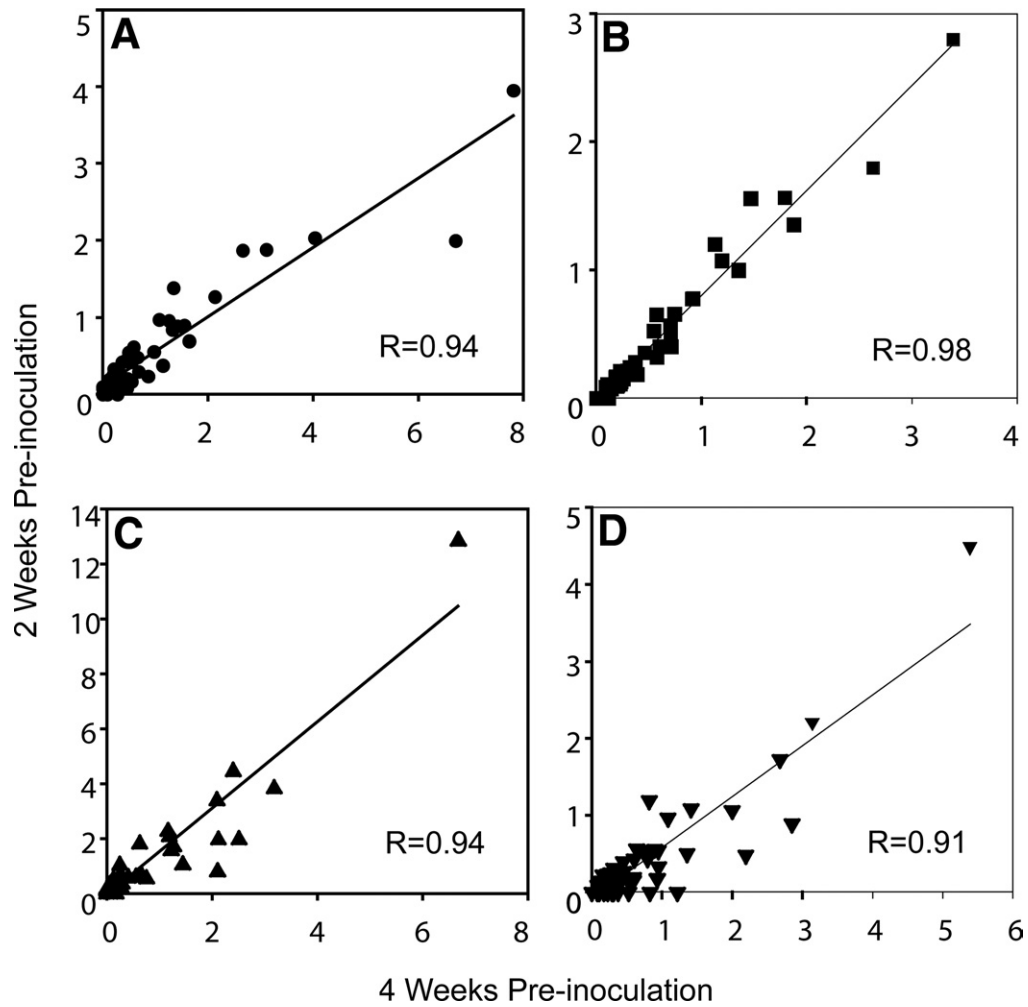
**Supplementary Table 1.** Comparison of Oligosaccharide Mass, Composition, and Frequency in Antral Gastric Biopsies of Humans and Monkeys Without *H pylori* Infection<sup>a,b,c</sup>

	m/z [M+Na]	OS composition			Frequency (%)	
		Hex	HexNAc	Fucose	Human	Monkey
<sup>a</sup> Group I	611.228	1	2	0	100	100
	773.280	2	2	0	100	100
	814.307	1	3	0	100	100
	919.338	2	2	1	100	100
	960.365	1	3	1	100	100
	976.360	2	3	0	100	100
	1065.396	2	2	2	100	100
	1122.418	2	3	1	100	100
	1138.413	3	3	0	100	100
	1179.439	2	4	0	100	100
	1268.476	2	3	2	100	100
	1284.470	3	3	1	100	100
	1325.497	2	4	1	100	100
	1341.492	3	4	0	100	100
	1430.528	3	3	2	100	100
	1487.550	3	4	1	100	100
	1544.571	3	5	0	100	100
	1633.608	3	4	2	100	100
	1690.629	3	5	1	100	100
	1795.661	4	4	2	100	100
1852.682	4	5	1	100	100	
1941.718	4	4	3	100	100	
1998.740	4	5	2	100	100	
<sup>b</sup> Group II	757.285	1	2	1	100	88
	1227.449	3	2	2	100	88
	1471.555	2	4	2	100	88
	1576.586	3	3	3	100	88
	1836.687	3	5	2	100	88
	1779.666	3	4	3	100	75
	2144.798	4	5	3	100	63
	2201.819	4	6	2	100	38
	1747.651	3	6	0	100	0
	2055.761	4	6	1	100	0
	2087.776	4	4	4	100	0
	1982.745	3	5	3	88	50
	1373.507	3	2	3	88	0
	1617.613	2	4	3	88	0
	2290.856	4	5	4	88	0
	2452.909	5	5	4	75	50
	1211.454	2	2	3	75	0
	2233.834	4	4	5	75	0
	1414.533	2	3	3	63	0
	2598.966	5	5	5	63	0
	2509.930	5	6	3	50	38
	554.206	1	1	1	50	0
	1925.724	3	4	4	50	0
	2347.877	4	6	3	50	0
	2655.988	5	6	4	38	13
	1763.671	2	4	4	38	0
	1900.692	5	3	3	38	0
1366.524	1	5	1	25	0	
1535.560	4	2	3	25	0	
1731.656	2	6	1	25	0	
1884.697	4	3	4	25	0	
2046.750	5	3	4	25	0	
2745.024	5	5	6	25	0	
408.148	1	1	0	13	0	

**Supplementary Table 1.** (Continued)

	m/z [M+Na]	OS composition			Frequency (%)	
		Hex	HexNAc	Fucose	Human	Monkey
	1097.386	4	2	0	13	0
	1243.444	4	2	1	13	0
	1300.465	4	3	0	13	0
	1389.502	4	2	2	13	0
	1512.582	1	5	2	13	0
	1608.576	5	3	1	13	0
	1754.634	5	3	2	13	0
	1868.702	3	3	5	13	0
	2112.782	4	7	0	13	0
	2265.824	6	4	3	13	0
	2395.887	5	4	5	13	0
	2427.877	7	4	3	13	0
	2557.940	6	4	5	13	0
	2573.935	7	4	4	13	0
	2630.956	7	5	3	13	0
	2964.099	6	6	5	13	0
<sup>c</sup> Group III	1081.391	3	2	1	88	100
	1649.603	4	4	1	88	100
	1592.581	4	3	2	50	100
	1017.386	1	4	0	38	100
	1446.523	4	3	1	25	100
	1503.545	4	4	0	25	100
	1738.639	4	3	3	25	100
	1811.656	5	4	1	13	100
	1957.713	5	4	2	13	100
	1382.519	2	5	0	0	100
	935.333	3	2	0	38	88
	2306.851	5	5	3	75	88
	2103.771	5	4	3	13	88
	2014.735	5	5	1	50	83
	2160.793	5	5	2	50	83
	1528.577	2	5	1	25	75
	1893.709	3	6	1	0	75
	1706.624	4	5	0	38	63
	2363.872	5	6	2	25	63
	2249.829	5	4	4	13	63
2322.846	6	5	2	13	50	
2468.904	6	5	3	13	50	
449.175	0	2	0	13	38	
2614.961	6	5	4	13	38	
2671.983	6	6	3	0	25	
2818.041	6	6	4	0	25	
2525.925	6	6	2	0	13	
2566.952	5	7	2	0	13	

<sup>a</sup>Oligosaccharides detected in 100% of monkeys and humans.<sup>b</sup>Oligosaccharides with higher detection frequency in humans.<sup>c</sup>Oligosaccharides with higher detection frequency in monkeys.



**Supplementary Figure 3.** Reproducibility of glycan profiles generated from the same monkey at 2 time points prior to inoculation with *H. pylori*. Correlation was calculated from absolute peak intensities using Pearson  $r$ .

**Supplementary Table 2.** Neutral Oligosaccharide Mass, Composition, and Frequency of Detection in Antral Gastric Biopsy Samples From 4 Rhesus Monkeys Pre- and Post-*H pylori* Infection<sup>a,b</sup>

Group	m/z [M+Na]	OS composition			Frequency (%)				
		Hex	HexNAc	Fucose	Pre		Post		
					-4 wk	-2 wk	2 wk	8 wk	24 wk
<sup>a</sup> Group I	408.148	1	1	0	100	100	0	0	100
	449.175	0	2	0	100	100	0	0	100
	773.280	2	2	0	100	100	0	0	75
	1341.492	3	4	0	100	100	0	0	75
	1446.523	4	3	1	100	100	0	0	75
	1503.545	4	4	0	100	100	0	0	75
	1544.571	3	5	0	100	100	0	0	75
	1592.581	4	3	2	100	100	0	0	75
	1690.629	3	5	1	100	100	0	0	75
	1852.682	4	5	1	100	100	0	0	75
	1998.740	4	5	2	100	100	0	0	75
	1957.713	5	4	2	100	100	0	0	50
	2103.771	5	4	3	100	100	0	0	50
	2160.793	5	5	2	100	100	0	0	50
	2468.904	6	5	3	100	50	0	0	25
	1528.577	2	5	1	75	75	0	0	75
	1836.687	3	5	2	75	100	0	0	75
	1893.709	3	6	1	75	75	0	0	75
	1811.656	5	4	1	75	100	0	0	50
	2014.735	5	5	1	75	100	0	0	50
	935.333	3	2	0	75	75	0	0	50
	2144.798	4	5	3	75	75	0	0	50
	1982.745	3	5	3	75	50	0	0	50
	2818.041	6	6	4	75	50	0	0	50
	2322.846	6	5	2	75	50	0	0	25
	2363.872	5	6	2	75	50	0	0	25
	2509.930	5	6	3	75	25	0	0	25
	2614.961	6	5	4	75	25	0	0	25
	1706.624	4	5	0	50	50	0	0	25
	2201.819	4	6	2	50	50	0	0	25
	2525.925	6	6	2	50	25	0	0	25
	2671.983	6	6	3	50	25	0	0	25
	2655.988	5	6	4	50	0	0	0	25
	2834.036	7	6	3	25	0	0	0	25
	2980.094	7	6	4	25	0	0	0	25
	2566.952	5	7	2	25	0	0	0	0
	2713.010	5	7	3	25	0	0	0	0
	1471.555	2	4	2	75	75	0	25	75
	1325.497	2	4	1	100	100	25	0	75
	1649.603	4	4	1	100	100	25	0	75
1738.639	4	3	3	100	100	25	0	50	
1941.719	4	4	3	100	100	25	0	50	
2306.851	5	5	3	100	100	25	0	50	
1779.666	3	4	3	75	75	25	0	50	
2249.829	5	4	4	75	75	25	0	50	
2452.909	5	5	4	75	50	25	0	50	
1017.386	1	4	0	100	100	25	25	75	
<sup>b</sup> Group II	1081.391	3	2	1	100	100	0	50	75
	757.286	1	2	1	100	75	0	50	75
	960.365	1	3	1	50	100	0	50	75
	611.228	1	2	0	100	100	0	75	75
	1576.586	3	3	3	75	100	25	50	50
	919.338	2	2	1	100	100	25	75	75
	1382.519	2	5	0	100	100	50	0	75
	1795.661	4	4	2	100	100	50	25	75
	1268.476	2	3	2	100	100	50	50	75
	1487.550	3	4	1	100	100	50	50	75
	1227.449	3	2	2	100	75	50	75	75

**Supplementary Table 2.** (Continued)

Group	m/z [M+Na]	OS composition					Frequency (%)				
		OS composition			Pre		Post				
		Hex	HexNAc	Fucose	-4 wk	-2 wk	2 wk	8 wk	24 wk		
	1065.396	2	2	2	75	100	50	75	75		
	976.360	2	3	0	100	100	75	25	75		
	1138.413	3	3	0	100	100	75	25	75		
	1633.608	3	4	2	100	100	75	25	75		
	814.307	1	3	0	100	100	75	50	75		
	1122.418	2	3	1	100	100	75	75	75		
	1179.439	2	4	0	100	100	75	75	75		
	1430.528	3	3	2	100	100	75	75	75		
	1284.471	3	3	1	100	100	100	75	75		

<sup>a</sup>Oligosaccharides detected in  $\leq 25\%$  of monkeys at 2 and 8 weeks postinfection.

<sup>b</sup>Oligosaccharides detected in  $\geq 50\%$  of monkeys at 2 and 8 weeks postinfection.

**Supplementary Table 3.** Acidic Oligosaccharide Mass, Composition, and Frequency of Detection in Antral Gastric Biopsy Samples From 4 Monkeys Pre- and Postinfection With *H pylori*

m/z [M+Na]	OS composition						Frequency (%)				
	OS composition						Pre		Post		
	Hex	HexNAc	Fucose	NeuAc	NeuGc	Na	-4 wk	-2 wk	2 wk	8 wk	24 wk
1207.3839	4	1	0	1	0	2	0	50	0	0	75
1264.4054	3	2	0	0	1	2	50	75	0	0	100
1410.4633	4	2	0	1	0	2	50	50	0	0	75
1410.4633	3	2	1	0	1	2	50	50	0	0	75
1426.4582	4	2	0	0	1	2	75	100	0	0	75
1572.5161	5	2	0	1	0	2	75	75	0	0	50
1572.5161	4	2	1	0	1	2	75	75	0	0	50
1825.6589	1	5	2	1	0	2	75	75	0	0	75
1825.6589	0	5	3	0	1	2	75	75	0	0	75

**Supplementary Table 4.** Oligosaccharide Mass, Composition, and Frequency of Detection in Antral Gastric Mucosa of Humans With (Hp+) or Without (Hp-) *H pylori* Infection

m/z [M+Na]	OS composition			Frequency (%) <sup>a</sup>	
	Hex	HexNAc	Fucose	Hp+	Hp-
611.228	1	2	0	100	100
757.285	1	2	1	100	100
773.280	2	2	0	100	100
814.307	1	3	0	100	100
919.338	2	2	1	100	100
976.360	2	3	0	100	100
1065.396	2	2	2	100	100
1122.418	2	3	1	100	100
1138.413	3	3	0	100	100
1179.439	2	4	0	100	100
1268.476	2	3	2	100	100
1284.470	3	3	1	100	100
1325.497	2	4	1	100	100
1341.492	3	4	0	100	100
1430.528	3	3	2	100	100
1471.555	2	4	2	100	100
1487.550	3	4	1	100	100
1544.571	3	5	0	100	100
1576.586	3	3	3	100	100
1633.608	3	4	2	100	100
1690.629	3	5	1	100	100
1722.644	3	3	4	100	100
1779.666	3	4	3	100	100
1795.661	4	4	2	100	100
1836.687	3	5	2	100	100
1852.682	4	5	1	100	100
1941.718	4	4	3	100	100
1998.740	4	5	2	100	100
2055.761	4	6	1	100	100
2087.776	4	4	4	100	100
2144.798	4	5	3	100	100
2201.819	4	6	2	100	100
1649.603	4	4	1	100	88
2290.856	4	5	4	100	88
2233.834	4	4	5	100	75
2306.851	5	5	3	100	75
2452.909	5	5	4	100	75
2598.966	5	5	5	100	63
1747.651	3	6	0	89	100
1373.507	3	2	3	89	88
1211.454	2	2	3	89	75
2160.793	5	5	2	89	50
2347.877	4	6	3	89	50
1982.745	3	5	3	78	88
1414.533	2	3	3	78	63
1925.724	3	4	4	78	50
2509.930	5	6	3	78	50
2014.735	5	5	1	67	50
2655.988	5	6	4	67	38
1738.639	4	3	3	67	25
2112.783	4	7	0	67	13
1617.613	2	4	3	67	88
1227.449	3	2	2	67	100
1382.519	2	5	0	56	0
1081.391	3	2	1	56	88
960.365	1	3	1	56	100
1706.624	4	5	0	44	38

**Supplementary Table 4.** (Continued)

m/z [M+Na]	OS composition			Frequency (%) <sup>a</sup>	
	Hex	HexNAc	Fucose	Hp+	Hp-
1884.697	4	3	4	44	25
2745.024	5	5	6	33	25
1893.709	3	6	1	33	0
1017.386	1	4	0	22	38
1900.692	5	3	3	22	38
1446.523	4	3	1	22	25
2363.872	5	6	2	22	25
2103.771	5	4	3	22	13
2249.829	5	4	4	22	13
2964.099	6	6	5	22	13
2713.009	5	7	3	22	0
2818.041	6	6	4	22	0
1592.581	4	3	2	11	50
935.333	3	2	0	11	38
1503.545	4	4	0	11	25
2046.750	5	3	4	11	25
1300.465	4	3	0	11	13
1754.634	5	3	2	11	13
1811.655	5	4	1	11	13
1868.702	3	3	5	11	13
1957.713	5	4	2	11	13
2630.956	7	5	3	11	13
2379.892	4	4	6	11	0
2566.952	5	7	2	11	0
2671.983	6	6	3	11	0
1763.671	2	4	4	0	38
1366.524	1	5	1	0	25
1528.576	2	5	1	0	25
1535.560	4	2	3	0	25
1731.656	2	6	1	0	25
1097.386	4	2	0	0	13
1243.444	4	2	1	0	13
1389.502	4	2	2	0	13
1512.582	1	5	2	0	13
1608.576	5	3	1	0	13
2265.824	6	4	3	0	13
2322.846	6	5	2	0	13
2395.887	5	4	5	0	13
2427.877	7	4	3	0	13
2468.903	6	5	3	0	13
2557.940	6	4	5	0	13
2573.935	7	4	4	0	13
2614.961	6	5	4	0	13

<sup>a</sup>Sorted by Hp+ frequency (%).